# Spiral-plane flop probed by ESR in the multiferroic triangular-lattice antiferromagnet $CuCrO_2$

H. Yamaguchi,[1] S. Ohtomo,[1] S. Kimura,[1] M. Hagiwara,[1] K. Kimura,[2] T. Kimura,[2] T. Okuda,[3,4] and K. Kindo[5]
[1]*KYOKUGEN, Osaka University, Machikaneyama 1-3, Toyanaka 560-8531, Japan*
[2]*Division of Materials Physics, Graduate School of Engineering Science, Osaka University, Toyonaka, Osaka 560-8531, Japan*
[3]*Department of Nano-Structures and Advanced Materials, Kagoshima University, 1-21-40 Korimoto, Kagoshima 890-0065, Japan*
[4]*PRESTO, JST, 4-1-8 Honcho, Kawaguchi, Saitama 332-0012, Japan*
[5]*Institute for Solid State Physics, University of Tokyo, 5-1-5 Kashiwanoha, Kashiwa, Chiba 277-8581, Japan*
(Received 29 September 2009; revised manuscript received 12 December 2009; published 15 January 2010)

We have performed high-field multifrequency electron spin resonance and magnetization measurements in magnetic field $H$ up to about 53 T on single crystals of a multiferroic triangular-lattice antiferromagnet $CuCrO_2$. We observed that one of the resonance modes showed a discontinuous change around 5.3 T for $H \| [1\bar{1}0]$, where the system undergoes a first-order phase transition accompanying a remarkable magnetoelectric effect. We explain the observed anomaly quantitatively in terms of the spiral-plane flop, considering a distorted triangular-lattice model with two kinds of antiferromagnetic in-plane exchange interactions and rhombic anisotropy.

DOI: 10.1103/PhysRevB.81.033104 PACS number(s): 76.50.+g, 75.50.Ee, 75.80.+q

Recent discoveries of new classes of multiferroics have attracted much attention due to intense interests in their microscopic origins and the possibility of their applications.[1–4] It is worth noting that some of them are reported to show ferroelectricity driven by spiral-spin orders and giant magnetoelectric (ME) effects attributed to the flops of the ferroelectric polarization by the application of magnetic fields, and those effects are confirmed to be accompanied by the flops of the spin spiral-plane being first-order phase transitions.[5–8] The control of ferroelectricity by magnetic fields is quite important for new spin-based device applications. However, there have been few quantitative approaches to the magnetic origin of the ferroelectric polarization and spiral-plane flops. First-order phase transitions in magnetic fields on spiral-spin structures have well investigated theoretically by Nagamiya *et al.*[9] Transition fields are considered to be sensitive to anisotropy energy.[9] Therefore, quantitative explanations of spiral-plane flops are expected to provide significant information about anisotropy related to the ME effects in these multiferroics.

Very recently, a flop of ferroelectric polarization by applying a magnetic field $H$ was found in a multiferroic triangular-lattice antiferromagnet (TLA), $CuCrO_2$, in which the $Cr^{3+}$ ions ($3d^3$, $S=3/2$) form an equilateral triangular lattice in the $c$ plane at room temperature.[10] The TLA having the delafossite structure shows successive magnetic transitions at $T_{N1}=23.6$ K and $T_{N2}=24.2$ K and ferroelectricity with the electric polarization $P$ parallel to the $c$ plane below $T_{N1}$.[11,12] An early powder neutron diffraction study proposed that the ground state of $CuCrO_2$ exhibits an out-of-plane 120° spin structure.[13] A recent neutron powder diffraction study indicated an out-of-plane incommensurate spiral-spin structure with an in-plane wave vector $\boldsymbol{q}=(0.329,0.329,0)$ below $T_{N1}$,[14] corresponding to the 118° spiral-spin structure. A polarized neutron-diffraction measurements on single crystals revealed that the spiral plane is parallel to the (110) plane.[15] The flop of $P$ is observed in the spiral-spin ordered phase by applying a magnetic field along the $[1\bar{1}0]$ direction.[10] At temperatures much below $T_{N1}$, the field derivative of magnetization ($dM/dH$) indicates a distinct peak structure with hysteresis at $H_c \sim 5.3$ T.[10] In accordance with the magnetic anomaly, the direction of $P$ is flopped from the [110] to the $[1\bar{1}0]$ direction. Taking account of the magnetic symmetry, it has been proposed that the transition is attributed to the (110) spiral-plane flop into the $(1\bar{1}0)$ plane.[10]

To unravel the origin of the first-order phase transition accompanying the ferroelectric polarization flop in $CuCrO_2$, we carried out high-field multifrequency electron spin resonance (ESR) and magnetization measurements in magnetic field up to about 53 T on single crystals of $CuCrO_2$. By a mean-field analysis assuming a distorted triangular-lattice model with two kinds of antiferromagnetic in-plane exchange interactions and rhombic anisotropy, we successfully explain the frequency dependence of the ESR resonance fields and the magnetization curves below $T_{N1}$ and evaluate the anisotropy and the exchange interaction constants. Our results clearly show that the spiral-plane flop occurs in the low-temperature region for the $H \| [1\bar{1}0]$ configuration, which brings about the ferroelectric polarization flop. The results also demonstrate that the deformation of the triangular lattice inducing small but finite in-plane anisotropy plays a critical role in the flops of the spiral-plane and ferroelectric polarization in the multiferroic TLA.

The ESR measurements at frequencies up to 1.4 THz were conducted in pulsed magnetic fields up to about 53 T at 1.3 K. The ESR measurements below 500 GHz in steady magnetic fields up to 14 T at 1.4 K were done by utilizing a superconducting magnet and a vector network analyzer. High-field magnetization measurements in pulsed magnetic fields up to about 53 T were carried out with a nondestructive pulse magnet at 1.3 K. The magnetization was measured by an induction method using a pick-up coil. The magnetization at 2 K was measured also by using a superconducting quantum interference device magnetometer (Quantum Design MPMS-XL7, USA). Single crystals of $CuCrO_2$ used in this study were grown from $Bi_2O_3$ flux.[12]

Figures 1(a) and 1(b) show the frequency dependence of the ESR absorption spectra at 1.3 K in pulsed magnetic fields

 

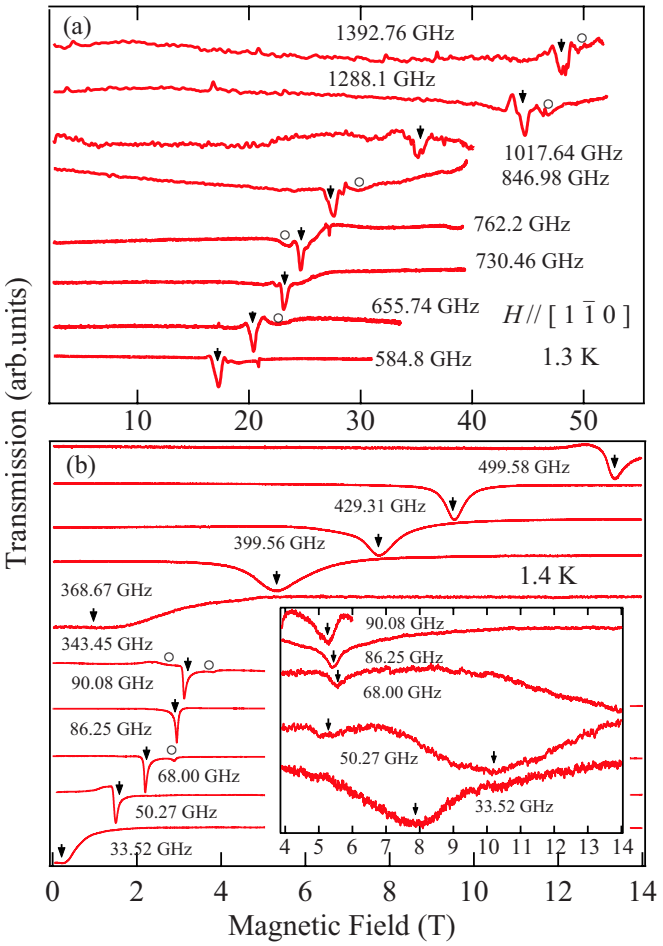


FIG. 1. (Color online) Frequency dependence of ESR absorption spectra of $CuCrO_2$ for $H\|[1\bar{1}0]$ (a) at 1.3 K in pulsed magnetic fields and (b) at 1.4 K in static magnetic fields. The arrows and circles indicate the strong and the weak signals, respectively. The inset of (b) shows the extended figure of the low-frequency ESR spectra observed above $H_c$ where a spiral-plane flop takes place.

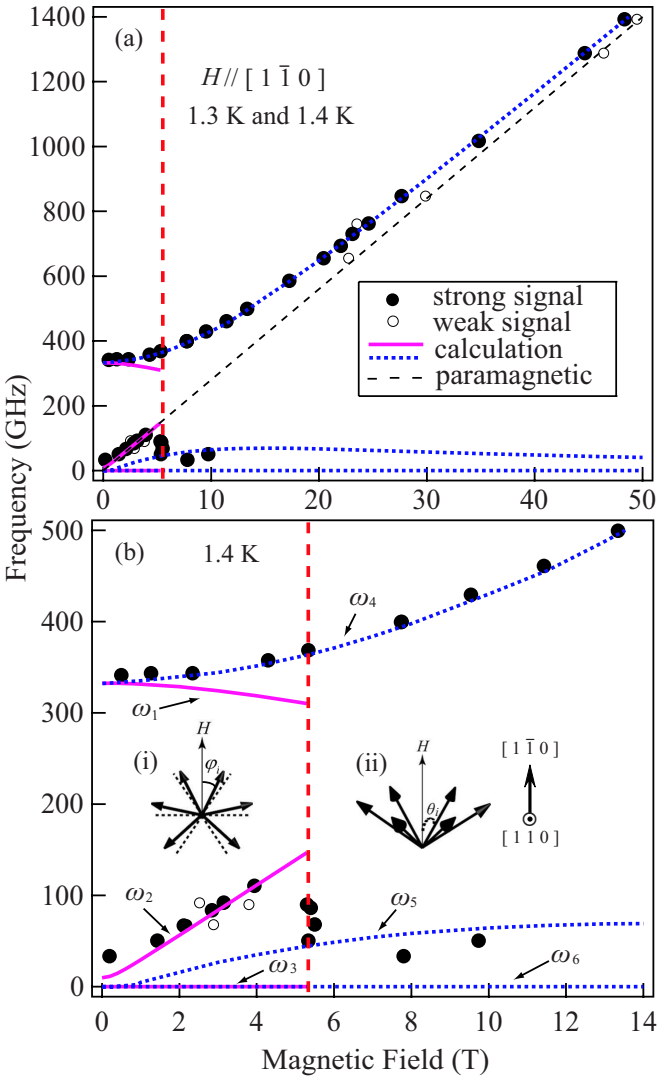


FIG. 2. (Color online) (a) Frequency-field diagram of $CuCrO_2$ at 1.3 and 1.4 K for $H\|[1\bar{1}0]$. (b) The extended figure below 500 GHz. Closed and open circles denote strong and weak signals, respectively. Solid and short broken lines show the calculated ESR modes. The thin broken line represents a paramagnetic-resonance line. The broken vertical line shows $H_c$, and the illustrations show schematic views of spin configuration in an external magnetic field.

and at 1.4 K in static magnetic fields for $H\|[1\bar{1}0]$, respectively. We observe strong resonance signals indicated by the arrows and a few weak signals indicated by the open circles. Since the resonance fields of the weak signals are very close to those of the strong ones and almost proportional to the external fields, we consider that they arise from a few crystal mosaics or paramagnetic centers caused by imperfections in the lattices. All resonance fields are plotted on the frequency-field plane in Fig. 2. There are two kinds of ESR modes with zero-field gaps about 340 and 30 GHz. The low-frequency resonance mode shows an obvious change around $H_c$=5.3 T, where the first-order phase transition occurs. Figure 3 shows a magnetization process at 1.3 K in a pulsed magnetic field for $H\|[1\bar{1}0]$. The magnetization increases almost linearly with increasing field for the whole range of applied magnetic fields. The inset (a) of Fig. 3 shows the $dM/dH$ curve observed in a static field at 2 K for $H\|[1\bar{1}0]$. The $dM/dH$ shows a distinct peak around $H_c$, as reported previously.[10]

We discuss the frequency dependence of the ESR resonance fields. Recent magnetostriction measurements[16] showed that there is a slight distortion of the hexagon with shrinkage along the [110] and stretch along the $[1\bar{1}0]$ in the low-temperature region as shown in Fig. 4(a). Thus, it is expected that there are two kinds of exchange interactions, $J_1$ and $J_2(J_1>J_2)$, in the $c$ plane below $T_{N1}$ as shown in Fig. 4(a). We consider that the incommensurability in the spin structure of $CuCrO_2$, suggested by the neutron-diffraction measurement,[14] is related to the inequivalence between $J_1$ and $J_2$. The interplane exchange interaction is neglected here for simplicity. In that case, conventional mean-field approximation theory gives that the exchange constants are required to be $J_2/J_1$=0.95 to realize the 118° spiral-spin structure. In addition, we need to take into account not only an easy-axis-type anisotropy, which stabilizes the out-of-plane spiral-spin

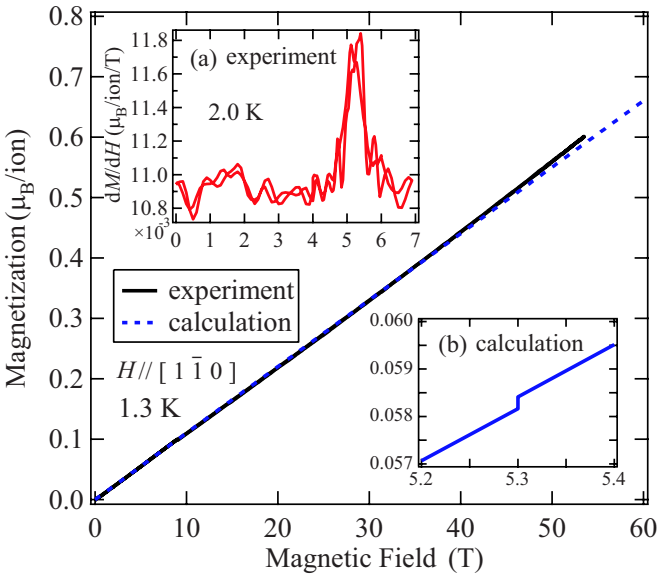


FIG. 3. (Color online) Magnetization process of $CuCrO_2$ at 1.3 K for $H \| [1\bar{1}0]$. Solid and broken lines are experimental and calculated results, respectively. Inset: (a) the derivative of the observed magnetization with respect to the field at 2 K. (b) The extended figure of calculated magnetization around $H_c$.

structure, but also an in-plane anisotropy for the explanations of the experimental results. Thus the spin Hamiltonian for the distorted triangular lattice is written as

$$\mathcal{H} = J_1 \sum_{\langle ij \rangle} \boldsymbol{S}_i \cdot \boldsymbol{S}_j + J_2 \sum_{\langle lm \rangle} \boldsymbol{S}_l \cdot \boldsymbol{S}_m + D \sum_i (S_i^z)^2 + E \sum_i \{(S_i^x)^2 - (S_i^y)^2\} - g\mu_B \sum_i \boldsymbol{S}_i \cdot \boldsymbol{H}, \quad (1)$$

where $D$ is the out-of-plane anisotropy of the easy-axis type ($D<0$), $E$ the in-plane anisotropy ($E>0$), $\mu_B$ the Bohr magneton, $\boldsymbol{H}$ the external magnetic field, $\langle ij \rangle$ and $\langle lm \rangle$ all the corresponding nearest-neighbor pairs, and the $x$, $y$, and $z$ axes are defined to be parallel to the [110], $[1\bar{1}0]$, and [001] axes, respectively. The 118° spiral-spin structure can be described by 180 sublattices model. Then the free energy $F$ is expressed by the following form using a mean-field approximation:

$$F = K \sum_{\langle ij \rangle} \boldsymbol{M}_i \cdot \boldsymbol{M}_j + L \sum_{\langle lm \rangle} \boldsymbol{M}_l \cdot \boldsymbol{M}_m + P \sum_{i=1}^{180} (M_i^z)^2 + Q \sum_{i=1}^{180} \{(M_i^x)^2 - (M_i^y)^2\} - \sum_{i=1}^{180} \boldsymbol{M}_i \cdot \boldsymbol{H}, \quad (2)$$

where $K=180J_1/[N(g\mu_B)^2]$, $L=180J_2/[N(g\mu_B)^2]$, $P=180D/[N(g\mu_B)^2]$, $Q=180E/[N(g\mu_B)^2]$, and $\boldsymbol{M}_i = Ng\mu_B \boldsymbol{S}_i/180$. $N$ is the number of magnetic ions and $\boldsymbol{S}_i$ is the spin on the $i$th sublattice. We derive the resonance conditions by solving the equation of motion

$$\partial \boldsymbol{M}_i / \partial t = \gamma [\boldsymbol{M}_i \times \boldsymbol{H}_i], \quad (3)$$

where $\gamma$ is the gyromagnetic ratio and $\boldsymbol{H}_i$ is a mean field applied on the $i$th sublattice moment given by

$$\boldsymbol{H}_i = -\partial F / \partial \boldsymbol{M}_i. \quad (4)$$

To solve the equation of motion, we use a method applied for $ABX_3$-type antiferromagnets.[17] Assuming precession motions of the sublattice moments around those equilibrium directions, we utilize the following expressions, which represent the motion of the $i$th sublattice moment,

$$\boldsymbol{M}_i = [\Delta M_{i\acute{x}} \exp(i\omega t), \Delta M_{i\acute{y}} \exp(i\omega t), |M_i|], \quad (5)$$

where $\Delta M_{i\acute{x}}, \Delta M_{i\acute{y}} \ll |\boldsymbol{M}_i|$, and $\acute{x}$, $\acute{y}$, and $\acute{z}$ are the principal axes of the coordinate system on each sublattice moment. The $\acute{z}$ axis is defined to be parallel to the direction of the each sublattice moment and the $\acute{x}$ and $\acute{y}$ axes are perpendicular to that.

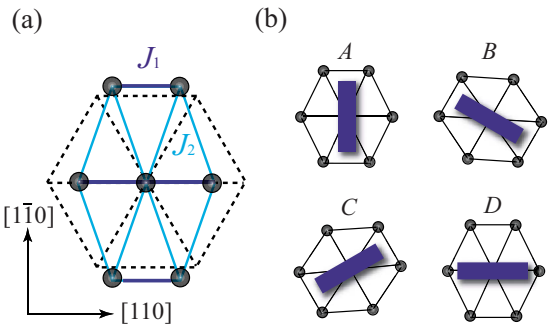


FIG. 4. (Color online) (a) The (001) projection of $Cr^{3+}$ trigonal layer. The broken and solid lines indicate hexagonal lattice and that with a slight distortion, respectively. (b) Schematic illustrations of spiral-plane domains. Thick lines denote the spiral plane. $A$, $B$, and $C$ are three degenerated domains at zero field. The $A$ domain shows the transition to the $D$ domain at $H_c$ for $H \| [1\bar{1}0]$.

The former experimental results and symmetry discussion suggest that three types of magnetic structure domains labeled $A$, $B$, and $C$ in Fig. 4(b) are stabilized in the low-temperature region at zero field,[18] and the domain $A$ suddenly flops into the domain $D$ at $H_c$ for $H \| [1\bar{1}0]$.[10] In the case of the domain $A$, we assume the distorted spin structure, in which spins lie in the (110) plane as shown by the schematic view (i) in Fig. 2(b). The distortion angles $\varphi_i$ are determined so as to minimize the energy of the assumed structure by solving differential equations $\partial F / \partial \varphi_i = 0 (i = 1-180)$, and we acquire them from numerical solutions. In the case of the domain $D$, we assume the so-called umbrella structure as shown by the schematic view (ii) in Fig. 2(b). The angles $\theta$ between each individual sublattice moment and the external field are also determined through the same procedure to determine $\varphi_i$ for the domain $A$. In the case of the domains $B$ and $C$, since their spiral planes are close to that of the domain $D$, we assume that the resonance modes for the domains $B$ and $C$ are the same as those of the domain $D$. The free energy of the domain $A$ becomes higher than that of the domain $D$ at a certain field $H_c$, where the first-order phase transition, corresponding to the spiral-plane flop, takes place. This transition occurs only for a finite $E$ value, which originates from a distortion of the crystal lattices. The value of $H_c$ mostly depends on the value of $E$ and has a relation

$H_c \propto \sqrt{E}$. We obtain good agreement between experiment and calculation as shown in Fig. 2 with the following parameter values: $J_1/k_B=28.0$ K, $J_2/k_B=26.6$ K, $D/k_B=0.47$ K, $E/k_B=0.0002$ K, and $g=2.0$, where the $g$ value is evaluated from the paramagnetic resonance at about 100 K. Below $H_c$, the domain $A$ shows two gapped modes, $\hbar\omega_1$ and $\hbar\omega_2$, and a gapless mode, $\hbar\omega_3=0$ and domains $B$ and $C$ also show two gapped modes, $\hbar\omega_4$ and $\hbar\omega_5$, and a gapless mode, $\hbar\omega_6=0$. At $H_c$, because of the spiral-plane flop transition from the domain $A$ to $D$, $\hbar\omega_1$ and $\hbar\omega_2$ abruptly change to $\hbar\omega_4$ and $\hbar\omega_5$, respectively. Moreover, ESR signals, corresponding to the critical-field resonance, are observed around $H_c$ as shown in the inset of Fig. 1(b). The signals for $\hbar\omega_1$ and $\hbar\omega_5$, however, are not observed. The reason is that the signal intensities of them are expected to be very weak due to the canceling of the transverse components of the sublattice moments. In addition, we calculated the magnetization process for the ground state at $T=0$ K by the mean-field theory using the same parameters determined by the ESR analyses. Then, we derived a small discontinuous change in the magnetization associated with the spiral-plane flop at $H_c$ as shown in the inset (b) of Fig. 3. Experimentally, no distinct anomaly is seen in the magnetization curve (the main panel of Fig. 3). However, the $dM/dH$ curve shows a clear peak around $H_c$ [the inset (a) of Fig. 3]. We consider that such a small jump of the magnetization is hardly observed owing to the finite-temperature effect. Our results strongly suggest that the electric-polarization flop observed in $CuCrO_2$ is attributed to the spiral-plane flop in only one of the three domains (domain $A$) and is sharply different from that in other multiferroics such as $TbMnO_3$ where the flop of $P$ comes from the flop of the entire cycloidal spiral-spin plane.[6] Very recently, a spin-polarized neutron study on $CuCrO_2$ confirmed that the domain $A$ shows the spiral-plane flop for $H\|[1\bar{1}0]$.[19]

In summary, we have performed high-field multifrequency ESR and magnetization measurements on single crystals of the multiferroic triangular-lattice antiferromagnet $CuCrO_2$. The frequency dependence of the ESR resonance fields and the magnetization process are well explained by a mean-field analysis considering the out-of-plane 118° spiral-spin structure on a distorted triangular-lattice model with two kinds of antiferromagnetic in-plane exchange interactions and rhombic anisotropy. Our results establish the benefits of ESR measurements combined with mean-field analyses to understand the origins of magnetoelectric effects in multiferroics, and also highlight the importance of lattice distortions caused by the spin-lattice coupling for first-order magnetic phase transitions in frustrated triangular-lattice antiferromagnets.

We thank K. Hirota and M. Soda for valuable discussion. This work was supported by Grants-in-Aid (Grants No. 17072005, No. 20340089, No. 2001004, and No. 20674005), and Global COE (Project No. G10) Programs of the Ministry of Education, Science, Sports, Culture and Technology in Japan.

[1] M. Fiebig, J. Phys. D **38**, R123 (2005).
[2] S.-W. Cheong and M. Mostovoy, Nature Mater. **6**, 13 (2007).
[3] D. Khomskii, Phys. **2**, 20 (2009).
[4] W. Eerenstein, N. D. Mathur, and J. F. Scott, Nature (London) **442**, 759 (2006).
[5] M. Fukunaga, Y. Sakamoto, H. Kimura, Y. Noda, N. Abe, K. Taniguchi, T. Arima, S. Wakimoto, M. Takeda, K. Kakurai, and K. Kohn, Phys. Rev. Lett. **103**, 077204 (2009).
[6] N. Aliouane, K. Schmalzl, D. Senff, A. Maljuk, K. Prokes, M. Braden, and D. N. Argyriou, Phys. Rev. Lett. **102**, 207205 (2009).
[7] K. Taniguchi, N. Abe, H. Umetsu, H. A. Katori, and T. Arima, Phys. Rev. Lett. **101**, 207205 (2008).
[8] S. Park, Y. J. Choi, C. L. Zhang, and S.-W. Cheong, Phys. Rev. Lett. **98**, 057601 (2007).
[9] T. Nagamiya, K. Nagata, and Y. Kitano, Prog. Theor. Phys. **27**, 1253 (1962).
[10] K. Kimura, H. Nakamura, S. Kimura, M. Hagiwara, and T. Kimura, Phys. Rev. Lett. **103**, 107201 (2009).
[11] S. Seki, Y. Onose, and Y. Tokura, Phys. Rev. Lett. **101**, 067204 (2008).
[12] K. Kimura, H. Nakamura, K. Ohgushi, and T. Kimura, Phys. Rev. B **78**, 140401(R) (2008).
[13] H. Kadowaki, H. Kikuchi, and Y. Ajiro, J. Phys.: Condens. Matter **2**, 4485 (1990).
[14] M. Poienar, F. Damay, C. Martin, V. Hardy, A. Maignan, and G. Andre, Phys. Rev. B **79**, 014412 (2009).
[15] M. Soda, K. Kimura, T. Kimura, M. Matsuura, and K. Hirota, J. Phys. Soc. Jpn. **78**, 124703 (2009).
[16] K. Kimura, T. Otani, H. Nakamura, Y. Wakabayashi, and T. Kimura, J. Phys. Soc. Jpn. **78**, 113710 (2009).
[17] H. Tanaka, Y. Kaahwa, T. Hasegawa, M. Igarashi, S. Teraoka, K. Iio, and K. Nagata, J. Phys. Soc. Jpn. **58**, 2930 (1989).
[18] Given spin chirality, there are twice as many domains (i.e., six domains). Here, however, we neglect the spin-chiral domains which cannot be distinguished by the present experiments.
[19] M. Soda and K. Hirota (private communication).